

See discussions, stats, and author profiles for this publication at: <https://www.researchgate.net/publication/224895384>

# Real-Time NMR Characterization of Structure and Dynamics in a Transiently Populated Protein Folding Intermediate

ARTICLE in JOURNAL OF THE AMERICAN CHEMICAL SOCIETY · MAY 2012

Impact Factor: 12.11 · DOI: 10.1021/ja302598j · Source: PubMed

---

CITATIONS

20

---

READS

60

6 AUTHORS, INCLUDING:



Enrico Rennella

University of Toronto

14 PUBLICATIONS 263 CITATIONS

SEE PROFILE



Paul Schanda

Institut de Biologie Structurale (IBS)

50 PUBLICATIONS 1,759 CITATIONS

SEE PROFILE

# Determining the Energy Landscape of Proteins by a Fast Isotope Exchange NMR Approach

Enrico Rennella,<sup>†</sup> Alessandra Corazza,<sup>†,§</sup> Luca Codutti,<sup>†</sup> Vittorio Bellotti,<sup>‡,§</sup> Monica Stoppini,<sup>‡,§</sup> Paolo Viglino,<sup>‡,§</sup> Federico Fogolari,<sup>‡,§</sup> and Gennaro Esposito<sup>\*,†,§</sup>

<sup>†</sup>Dipartimento di Scienze Mediche e Biologiche, Università di Udine, I-33100 Udine, Italy

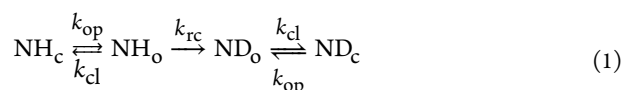
<sup>‡</sup>Dipartimento di Biochimica, Università di Pavia, I-27100 Pavia, Italy

<sup>§</sup>Istituto Nazionale Biostrutture e Biosistemi, I-00136 Rome, Italy

## S Supporting Information

**ABSTRACT:** We present a new and efficient NMR method, BLUU-Tramp (Biophysics Laboratory University of Udine temperature ramp), for the collection of hydrogen–deuterium exchange experiments as a function of time and temperature for small and medium-sized proteins. Exchange rates can be determined to extract the underlying thermodynamic equilibrium or kinetic parameters by sampling hundreds of points over a virtually continuous temperature ramp. Data are acquired in a single experimental session that lasts some 20–60 h, depending on the thermal stability of the protein. Subsequent analysis provides a complete thermodynamic description of the protein energy landscape. The global thermal unfolding process and the partial or local structure opening events can be fully determined at the single-residue resolution level. The proposed approach is shown to work successfully with the amyloidogenic protein  $\beta_2$ -microglobulin. With <sup>15</sup>N-labeling, the unfolding landscape of a protein can also be studied in the presence of other unlabeled proteins and, in general, with ligands or cosolutes or in physiological environments.

The study of isotope exchange in proteins has proven to be an extremely powerful tool for investigating the conformational equilibria that underlie the amide exchange kinetics.<sup>1–6</sup> The well-established general mechanism of amide exchange in polypeptide chains,<sup>1</sup>



dictates that amide hydrogens in a generic folded or closed (c) state must attain a generic unfolded or open (o) state before undergoing isotope exchange at the same rate as expected for a random coil (i.e.,  $k_{\text{rc}}$ ).<sup>3</sup> The relative magnitudes of the opening and closing rate constants  $k_{\text{op}}$  and  $k_{\text{cl}}$ , respectively, determine the position of the equilibrium between the open, exchange-competent and closed, exchange-incompetent states. This information is conveyed by the observed exchange rate

constant,  $k_{\text{ex}}$ , which, for folded peptides, adopts one of the two limiting forms<sup>1</sup>

$$k_{\text{ex}}^{\text{EX1}} \approx k_{\text{op}} \quad k_{\text{ex}}^{\text{EX2}} \approx \frac{k_{\text{op}}}{k_{\text{cl}}} \times k_{\text{rc}} \quad (2)$$

depending on whether  $k_{\text{rc}} \gg k_{\text{cl}}$  (EX1 regime) or  $k_{\text{rc}} \ll k_{\text{cl}}$  (EX2 regime). In the EX1 limit, the phenomenological  $k_{\text{ex}}$  value provides directly the kinetic constant of the opening event, which reports the lability of the closed state. In the EX2 limit, the measured  $k_{\text{ex}}$  value encodes the thermodynamic stability constant of the closed state, that can be extracted because the sequence-specific  $k_{\text{rc}}$  values are known.<sup>4</sup> Under intermediate conditions (i.e., the EXX limit<sup>6</sup>), extracting the previous information becomes more difficult, although it is still possible. The basic model of peptide hydrogen exchange (HX)<sup>1,2</sup> has been adapted to reflect more closely the conformational dynamics of proteins.<sup>4–6</sup> The opening events leading to HX correspond, in folded proteins, to global or partial unfolding processes that transform limited or extended populations of the native folded state (N) into the globally unfolded state (D) or a partially unfolded state (P) according to Boltzmann statistics.<sup>4–6</sup> If we simplify the description of the whole process at each NH by using a single opening process, the observed overall exchange rate can be simply written as

$$k_{\text{ex}}^{\text{EX1}} = k_{\text{ND}} \quad k_{\text{ex}}^{\text{EX2}} = \frac{k_{\text{ND}}}{k_{\text{DN}}} \times k_{\text{rc}} \quad (3)$$

where the EX1 or EX2 qualifications are borrowed from the regime of the global process and the subscripts ND and DN stand for the starting and final states of the considered event. Proteins that are in proximity of denaturation exchange almost exclusively by the EX1 regime, where the majority of amide HX is correlated, whereas far from denaturation, the EX2 regime dominates, with virtually no correlation among the individual amide HX rates.

NMR spectroscopy, and especially 2D NMR spectroscopy, is ideally suited for the study of HX in proteins, as it is the only technique that can monitor simultaneously the individual exchange processes for all of the resolved amide resonances of a protein. The statistical significance of a number of independent

Received: September 24, 2011

(identical or concurrent) kinetic sets, such as the NMR HX data, ensures the reliability for the fitting results. Hence, the unfolding processes that are enveloped in protein exchange data can be dissected into a single global event and, possibly, several partial ones.<sup>4</sup> To this aim, biophysicists usually record a series of 2D  $^1\text{H}$ – $^1\text{H}$  or  $^{15}\text{N}$ – $^1\text{H}$  experiments to follow the progress of the amide  $^1\text{H}$ – $^2\text{H}$  exchange as a function of time. The  $k_{\text{ex}}$  values of the individual residue amides are obtained by exponential fitting, and the associated thermodynamic or kinetic parameters are assessed according to eqs 3. Repeating the measurements at various temperatures allows the changes in the individual equilibrium and/or kinetic constants to be determined for subsequent analysis using the van't Hoff and/or Arrhenius equations, respectively. This leads to the extraction of enthalpy and entropy changes and/or activation energies for the unfolding processes for each resolved amide resonance, which represents the corresponding single backbone location. Identifying the global unfolding process means observing similar maxima (ideally equal, within the experimental error) of thermodynamic or activation parameters from a group of amides.<sup>7</sup> The observation of smaller values for the same parameters from the remaining amides is the signature of additional openings that take place on an individual, local, or subglobal scale simultaneously with the global process; these can be analyzed using a more complex framework than the basic one expressed by eqs 3.<sup>4–6</sup> Thus, the simple occurrence of global and partial processes requires a two-component analysis for some amides [see the Supporting Information (SI)]. Even without entering such complexity, discerning which residues are involved in the global opening process means recognizing the structural determinants of a protein, which is very valuable information for the comprehension of the function and mechanism of action of the protein as well as for mutagenesis. For a two-state unfolding transition, linearity of the van't Hoff plots should be observed. When a sufficient number of temperature points have been collected, the observation of nonlinearity in the van't Hoff graphs is the hallmark of more complex mechanisms involving intermediates. In such contexts, however, reaching sufficient confidence for reliable conclusions is rather demanding in terms of NMR measurement time and analysis effort. For this reason, one resorts to optical spectroscopy studies (fluorescence, circular dichroism, UV absorption) or directly to microcalorimetric measurements. These alternatives are much less time-consuming, and the corresponding data are more quickly analyzed, at the cost of substantial loss of detail because only bulk information on the protein transitions is extracted. To retain the information richness and the superior insight provided by the NMR approach, we propose a method that reduces the acquisition of the series of experiments at different temperatures into a single series pair collected as a function of time and temperature. Briefly, the protein HX is measured by repeating twice, with the same sample, the serial collection of 2D NMR spectra while applying a thermal ramp. The first series of spectra is acquired by dissolving in  $\text{H}_2\text{O}$  the protein previously exchanged in heavy water ( $\text{D}_2\text{O}$ ) and recovered by lyophilization from the same solvent. The resulting intensity time course of the amide signals ( $I_{\text{raw}}$ ) includes the buildup due to the hydrogen back-exchange process and the (unwanted) contribution from the thermal dependence of spin relaxation. The second series of spectra is recorded at the end of the back-exchange process. In this case, the sampled intensities ( $I_{\text{ref}}$ ) include only the contribution from

the thermal dependence of spin relaxation. Therefore, the quantity used for subsequent analysis,

$$N = (I_{\text{ref}} - I_{\text{raw}})/I_{\text{ref}} \quad (4)$$

reflects only the effect of the isotopic exchange process, reverting the original buildup into a decay. Differential relaxation effects arising from particularly slow protonation of closely spaced amides should be quite limited.

The isotopic exchange undergone by the N species during a linear ramp of temperature can be described by a time-course function,  $N(t)$ , that accounts for the evolution of the initial signal amplitude  $N(0)$  as follows:

$$N(t) = N(0) \exp\left\{-\int_0^t k_{\text{ex}}[T(t')] \, dt'\right\} \quad (5)$$

This amounts to nesting the time dependence of the temperature [i.e.,  $T(t)$ ] in the temperature dependence of  $k_{\text{ex}}$  [i.e.,  $k_{\text{ex}}[T(t)]$ ]. These latter rate constants are obtained by fitting the experimental intensity time course with the function

$$N(t) = c \exp[a \exp(bt)] \quad (6)$$

where  $a$ ,  $b$ , and  $c$  are fitting parameters. By taking the negative of the first derivative with respect to time of the logarithm of eqs 5 and 6, we get the function for the exchange rate constants (for details, see the SI):

$$-\frac{d}{dt} \ln[N(t)] = k_{\text{ex}}(T) = -ab \exp[bt(T)] \quad (7)$$

The thermal dependence of the exchange rates is derived by expanding the right-hand side of eqs 3 according to the relative Arrhenius equations (see the SI). The resulting thermodynamic and kinetic parameters can be evaluated by grouping the amide sites that exchange under a correlated regime, that is, with equilibrium constants ( $k_{\text{ND}}/k_{\text{DN}}$ ) or rate constants ( $k_{\text{ND}}$ ) for opening that prove to be very similar or equal within the experimental error. A more accurate procedure, explicitly accounting for global and partial opening processes, would entail a clustering analysis at this step. Such an analysis will be reported elsewhere, but the physical insight and power of our method is preserved also with the simplified scheme illustrated here and further extended in the SI. This is shown by the results obtained with human  $\beta_2$ -microglobulin ( $\beta_2\text{-m}$ ), an 11.7 kDa protein that occurs as non-polymorphic component of class-I major histocompatibility complex (MHC), which forms amyloid deposits in the joints of patients receiving hemodialysis treatment because of chronic renal failure.<sup>8</sup> Besides the NMR assignments and structure,<sup>9,10</sup> the results of a classical NMR HX study as a function of temperature are available for  $\beta_2\text{-m}$ <sup>11</sup> to draw comparisons. A 0.6 mM (U-98%  $^{15}\text{N}$ )  $\beta_2\text{-m}$  solution was pre-exchanged twice for 60 h at ambient temperature and lyophilized in  $\text{D}_2\text{O}$  containing 7 mM phosphate and 10 mM NaCl. The pre-exchanged powder was then dissolved in 93:7 (v/v)  $\text{H}_2\text{O}/\text{D}_2\text{O}$  buffer to give final phosphate and salt concentrations of 70 and 100 mM, respectively, at pH 6.44 (measured after data acquisition). Two series of  $^1\text{H}$ – $^{15}\text{N}$  SOFAST-HMQC<sup>12</sup> spectra were recorded as a function of temperature to sample first back-exchange and then reference intensities. The acquisition of each 2D spectrum lasted  $\sim 8$  min. An automated acquisition procedure was issued by standard Bruker software tools to alternate data collection and temperature ramp execution. The latter consisted of 0.1 K increments and equilibration intervals of 20 s over the range

295–315 K. NMR data processing was performed using NMRPipe.<sup>13</sup> Figure 1 shows the maps reporting the time–

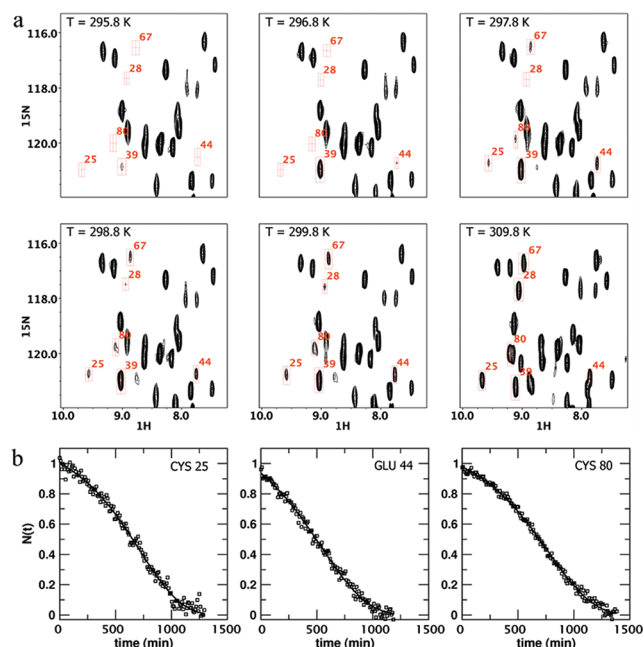


**Figure 1.** (a) Evolution of a specific region of the  $^1\text{H}$ – $^{15}\text{N}$  SOFAST-HMQC<sup>12</sup> spectrum of  $\beta 2$ -m in the HX experiment as a function of time and temperature. A few amide resonances that were well-resolved throughout the whole experiment are boxed, and their residue number assignments are indicated. All of the NMR experiments were performed on a Bruker Avance 500 spectrometer with triple-axis gradient coils (for additional details, see the SI). (b) Fitting of the experimental amide resonance intensities from the indicated residues according to eq 6. The time-course function  $N(t)$  is related to  $k_{\text{ex}}(T)$  through eq 7.

temperature dependence of a group of  $\beta 2$ -m amides along with the relative fitting to extract the  $k_{\text{ex}}(T)$  curves according to eqs 6 and 7. A C-written routine (available on request) was used for this purpose; it enabled direct calculation of the thermodynamic parameters starting from the experimental kinetic data in the EX2 limit.

Under the selected experimental conditions over the range 295–309 K, the  $\beta 2$ -m HX data could be analyzed by a single EX2 process or by dissecting global and local processes (see the SI). Figure 2a illustrates the results obtained using the single EX2 model for a subset of residues with well-resolved amide signals over the whole experiment. Only the  $\Delta G$  values for the opening equilibrium ( $\Delta G_{\text{op}}$ ) are plotted in the histogram. The complete set of parameters, including the corresponding  $\Delta H_{\text{op}}$  and  $\Delta S_{\text{op}}$  values and result comparisons, is listed in the SI. Grouping of the highest values reported in Figure 2a leads to the selection of eight residues, namely, Asn24, Cys25, Tyr26, Leu40, Tyr66, Cys80, Arg81, and Asn83, for which an average  $\Delta G$  value of  $8.1 \pm 0.3$  kcal/mol at 298 K was calculated, with a spread within two standard deviations. This  $\Delta G$  value should express the protein stability with respect to the global unfolding. The result is equal, within the experimental error, to the analogous average  $\Delta G$  values of  $7.9 \pm 0.5$  and  $8.8 \pm 0.5$  kcal/mol at pH 6.27 and 7, respectively, obtained using the method presented here and the value of  $9.0 \pm 0.6$  kcal/mol at pH 6.6 (reading in  $\text{D}_2\text{O}$ ) obtained using the classical procedure.<sup>11</sup> Therefore, the proposed approach, which lowers

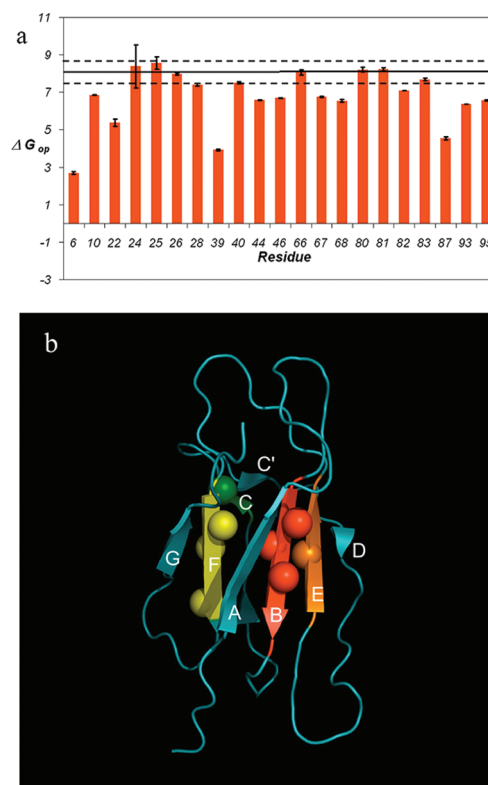


**Figure 2.** (a) Gibbs free energy differences (kcal/mol) at 298 K for the backbone opening equilibrium ( $\Delta G_{\text{op}}$ ) at specific  $\beta 2$ -m residues, as obtained after the individual  $k_{\text{ex}}(T)$  functions were determined from the intensity data. Numerical values and errors (reported on the bars) are listed in the SI. The horizontal line indicates the average  $\Delta G_{\text{op}}$  value ( $8.1 \pm 0.3$  kcal/mol) for a group of eight residues exhibiting highest  $\Delta G_{\text{op}}$  values and spreading within  $2\sigma$  (dashed lines). This average should correspond to the  $\Delta G$  value for global unfolding of the protein. (b)  $\beta 2$ -m structure (PDB entry 1JNJ<sup>10</sup>) highlighting the position of the eight residues (spheres) whose opening equilibria coincide with the global unfolding equilibrium. The cartoon was prepared with PyMOL (DeLano Scientific LLC).

by 1 order of magnitude the experimental time cost, is valid and reproducibly precise. The residues exhibiting the highest  $\Delta G_{\text{op}}$  values can be considered as structural determinants of the stability of the whole protein because their HX process should be exclusively driven by the global unfolding. In  $\beta 2$ -m, these residues, selected among those exhibiting the most reliable data, were found to be located in  $\beta$ -strands B, C, E, and F, that is, in the inner core of the immunoglobulin motif of the molecule (Figure 2b), with the exclusion of the edge strands (A, D, C', and G). Further gain in physical insight would be expected if the partial processes were explicitly taken into account.

This successful mapping of the structural determinants of a protein may be extended also to systems including protein interactors to assess and locate residues and regions responsible for thermodynamic differences due to stable complex or labile adduct formation. Proper labeling strategies may enable the application of the proposed 2D HX measurements in the presence of other proteins or cosolutes or in biological fluids. For the proposed method, HX is valuable when  $\Delta G > 5$  kcal/mol for the specifically relevant opening process, bearing in mind that the  $k_{\text{DN}}$  ( $k_{\text{cl}}$ ) value determines whether the EX1, EX2, or EXX regime dominates and that pH can be used to switch among these regimes. In principle, dimensions other



than temperature may be coupled to the HX kinetics to explore the effect of variables such as pH or chemical denaturant activity, and kinetics other than HX could be investigated. Besides the conspicuous experimental time reduction and the easy implementation with conventional instruments, pulse sequences, and processing, the use of a single sample avoids systematic errors from pH, buffer, and concentration differences and lowers the preparation costs. Finally, we are not unaware of the fact that the confidence level reached by the approach presented allows reliable conclusions to be drawn concerning the occurrence of intermediates along the unfolding pathway, although the determination of the actual pathway of the transformation may still remain uncertain.<sup>7</sup> The proposed method is dubbed BLUU-Tramp (Biophysics Laboratory University of Udine temperature ramp).

## ■ ASSOCIATED CONTENT

### 🔍 Supporting Information

Experimental details, equation transformations, and a table of thermodynamic parameters. This material is available free of charge via the Internet at <http://pubs.acs.org>.

## ■ AUTHOR INFORMATION

### Corresponding Author

rino.esposito@uniud.it

### Notes

The authors declare no competing financial interest.

## ■ ACKNOWLEDGMENTS

This work was supported by funds from Italian Ministry of University (PRIN-20083ERXWS, FIRB-RBRN07BMCT). The expert assistance of Dr. A. Makek is acknowledged.

## ■ REFERENCES

- (1) Hvidt, A.; Nielsen, S. O. *Adv. Protein Chem.* **1966**, *21*, 287.
- (2) Englander, S. W.; Kallenbach, N. R. *Q. Rev. Biophys.* **1983**, *16*, 521.
- (3) Bai, Y.; Milne, J. S.; Mayne, L.; Englander, S. W. *Proteins* **1993**, *17*, 75.
- (4) Bai, Y.; Sosnick, T. R.; Mayne, L.; Englander, S. W. *Science* **1995**, *269*, 192.
- (5) Marmorino, J. L.; Auld, D. S.; Betz, S. F.; Doyle, D. F.; Young, G. B.; Pielak, G. J. *Protein Sci.* **1993**, *2*, 1966.
- (6) Xiao, H.; Hoerner, J. K.; Eyles, S. J.; Dobo, A.; Voigtman, E.; Mel'čuk, A. I.; Kaltashov, I. A. *Protein Sci.* **2005**, *14*, 543.
- (7) Fersht, A. *Structure and Mechanism in Protein Science: A Guide to Enzyme Catalysis and Protein Folding*, 1st ed.; Freeman: New York, 1998.
- (8) Gejyo, F.; Yamada, T.; Odani, S.; Nakagawa, Y.; Arakawa, M.; Kunitomo, T.; Kataoka, H.; Suzuki, M.; Hirasawa, Y.; Shirahama, T.; Cohen, A. S.; Schmid, K. *Biochem. Biophys. Res. Commun.* **1985**, *129*, 701.
- (9) Okon, M.; Bray, P.; Vucelic, D. *Biochemistry* **1992**, *31*, 8906.
- (10) Verdone, G.; Corazza, A.; Viglino, P.; Pettirossi, F.; Giorgetti, S.; Mangione, P.; Andreola, A.; Stoppini, M.; Bellotti, V.; Esposito, G. *Protein Sci.* **2002**, *11*, 487.
- (11) Rennella, E.; Corazza, A.; Fogolari, F.; Viglino, P.; Giorgetti, S.; Stoppini, M.; Bellotti, V.; Esposito, G. *Biophys. J.* **2009**, *96*, 169.
- (12) Schanda, P.; Kupce, E.; Brutscher, B. *J. Biomol. NMR* **2005**, *33*, 199.
- (13) Delaglio, F.; Grzesiek, S.; Vuister, G. W.; Zhu, G.; Pfeifer, J.; Bax, A. *J. Biomol. NMR* **1995**, *6*, 277.